Erschienen in: Carbon ; 122 (2017). - S. 428-433
https://dx.doi.org/10.1016/j.carbon.2017.06.079

Growth and electronic structure of graphene on semiconducting Ge(110)

Julia Tesch [a], Elena Voloshina [b, *], Mikhail Fonin [a, **], Yuriy Dedkov [a, ***]

[a] Fachbereich Physik, Universität Konstanz, 78457 Konstanz, Germany
[b] Humboldt-Universität zu Berlin, Institut für Chemie, 10099 Berlin, Germany

A B S T R A C T

The direct growth of graphene on semiconducting or insulating substrates might help to overcome main drawbacks of metal-based synthesis, like metal-atom contaminations of graphene, transfer issues, etc. Here we present the growth of graphene on *n*-doped semiconducting Ge(110) by using an atomic carbon source and the study of the structural and electronic properties of the obtained interface. We found that graphene interacts weakly with the underlying Ge(110) substrate that keeps graphene's electronic structure almost intact promoting this interface for future graphene-semiconductor applications. The effect of dopants in Ge on the electronic properties of graphene is also discussed.

1. Introduction

Presently, the main synthesis methods of graphene (gr), a purely 2D material consisting of carbon atoms, which can be scaled down in order to be used in further applications, are its preparation on semiconducting SiC [1–3] or on metallic substrates [4–7]. However, these methods have natural drawbacks like, e. g., the price of the high-quality SiC wafers and very high processing temperature ($T > 1300^{\circ}$ C) used for the growth of the uniformly monolayer-thick homogeneous graphene on SiC [2,8]. In the case of graphene synthesis on metal substrates with subsequent transfer onto the desired support, it was found that the level of metal-atom contamination in the obtained graphene is not acceptable for modern microelectronics [9,10]. These as well as other fundamental problems limit the commercialization of graphene [11,12] and stimulate researchers to search for new ways of graphene synthesis.

One possibility to implement graphene in modern microelectronics processing is to perform its synthesis directly on an insulating substrate. Here one option is to use h-BN, which can be grown on the metallic substrates, like Cu, Fe, or Ni, or on semiconductors, like Ge, thus allowing a chemical vapour deposition (CVD) synthesis of graphene, furthermore to produce a tunnel barrier for the carrier injection in graphene, and to avoid a metal contamination of graphene [13–15]. Another approach implies a direct growth of graphene on the technologically relevant SiO_2/Si(001) substrate, that was successfully demonstrated recently [16].

A different method comprises graphene synthesis directly on a semiconducting substrate. The direct growth of graphene on Si is problematic due to its carbidic phase formation at high temperatures [17–21]. However, the recent progress in graphene synthesis reveals the possibility to grow single- and multilayer graphene on Ge and Ge/Si substrates [22–26]. While the Ge(001) surface is the most technologically relevant one, a faceting of the underlying Ge with the Ge(107) facets upon graphene growth was found by means of scanning electron and tunneling microscopy (SEM and STM) [25,27,28], which limits further technological processing of this interface. In contrast to the previous case, graphene as well as the underlying Ge surface remain flat for the Ge(110) surface, which was confirmed by low-energy electron diffraction (LEED) and STM [22,24,25]. Despite the availability of a number of intensive studies on the growth of graphene on Ge, little is known about the electronic structure of this interface [29]. In this work, the *ex situ* CVD

* Corresponding author.
** Corresponding author.
*** Corresponding author.
E-mail addresses: elena.voloshina@hu-berlin.de (E. Voloshina), mikhail.fonin@uni-konstanz.de (M. Fonin), yuriy.dedkov@uni-konstanz.de (Y. Dedkov).

grown graphene flakes on undoped Ge/Si(001) were investigated by means of micro- and nano-ARPES (angle-resolved photoelectron spectroscopy), which indicates the free-standing character of graphene maintaining the linear dispersion of the π states in the vicinity of the Fermi level (E_F) and its p-doping with the position of the Dirac point of $E_D = 0.185$ eV above E_F.

Here we present a complete *in situ* UHV preparation as well as a structural and electronic properties study of agraphene layer epitaxially grown from an atomic carbon source on Ge(110). The presented LEED and STM results confirm the high quality of the prepared system indicating the existence of a reconstructed Ge(110) surface below graphene. Our x-ray photoelectron spectroscopy (XPS), normal-emission ARPES (NE PES), and energy-loss near-edge spectroscopy performed at the carbon *K*-edge (C *K*-edge ELNES) reveal the nearly free-standing behaviour of graphene on Ge(110). We also address the plasmon excitations in this system performing electron-energy loss spectroscopy (EELS). Our results were compared and analyzed with the available theoretical spectroscopic data for free-standing graphene and "strongly-interacting" gr/Ni(111) demonstrating good agreement with the former case.

2. Experimental details

Growth of graphene and all studies were performed in the surface science cluster tool (Omicron NanoTechnology; base pressure 1×10^{-10} mbar). Prior to every experiment a Ge(110) substrate (G-materials (Germany), Sb doped, resistivity 0.35 Ω•cm) was cleaned via cycles of Ar^+-sputtering (1.5 keV, $p(\mathrm{Ar}) = 1 \times 10^{-5}$ mbar) and annealing ($T = 870^{\circ}$ C). Graphene was grown on the hot Ge(110) substrate ($T = 860 - 870^{\circ}$ C) from an atomic carbon source (Dr. Eberl MBE-Komponenten GmbH) with a filament current of $I =$ 70 A and maximum pressure of 2×10^{-9} mbar during C-deposition. The cleanliness and quality of the samples was controlled by LEED, STM (Omicron VT-SPM), NE PES (non-monochromatized He II line), and XPS (non-monochromatized Al *K* line; energy analyzer Omicron EA 125 was set either in angle-resolved or in angle-integrated mode, respectively) after every preparation step. ELNES and EELS experiments were performed in the specularly-reflected electron beam mode with angular and energy resolution of 1° and ≈1 eV, respectively. The primary electron energy is marked for every spectrum. Low-temperature (LT) STM experiments were performed in an Omicron Cryogenic STM on the gr/Ge(110) sample quickly transferred from the growth/characterization facility under N_2-atmosphere. Following the transfer, gr/Ge(110) was annealed in UHV at 700° C.

3. Results and discussions

The growth of graphene on Ge(110) was characterized by means of STM, LEED, and XPS and these results are compiled in Figs. 1 and 2. The Ge(110) surface shows a large scale ordering as can be deduced from the STM [Fig. 1 (a,b)] and LEED images [Fig. 1(f)]. According to previous studies this surface can be described as a faceted surface with {17 15 1} facets and $c(8 \times 10)$ reconstruction on the steps [30–33]. Deposition of carbon on Ge(110) at $T = 870^{\circ}$ C and subsequent cooling of the sample to room temperature lifts the previously observed reconstruction, however, producing an ordered underlying Ge surface as can be seen from the respective STM and LEED images [Fig. 1(c–e,g)].

The prepared graphene layer forms two types of domains rotated by 30° with respect to each other as seen from LEED and demonstrates a clear honeycomb sp^2 structure on the Ge(110) surface [Fig. 1(c–e,h)]. Our results on the observation of two graphene domains are consistent with the previously reported data for CVD grown graphene on Ge(110) [25]. The observed alignment of the graphene lattices of the two domains differs by ≈15° compared to the one observed for the single-domain graphene growth in Ref. [24]. Similar to the results presented in this reference, our growth method rules out the influence of hydrogen on the alignment of graphene on Ge(110); however, further structural studies, are required.

STM experiments performed on the large scale [Fig. 1(c and d)] and at different bias voltages [Fig. 1(e)] allow to obtain information on the thickness of a graphene layer and to resolve the atomic structure of graphene and the Ge(110) substrate underneath. A horizontal height profile taken across the STM image presented in panel (d) yields a height difference of ≈3.2 Å between the clean and graphene covered Ge(110) surface. This value is in very good agreement with the graphene–Ge-adatom distance of ≈3 Å obtained in the recent density functional theory (DFT) calculations for this system [24]. An average height of 3.7 – 3.8 Å between the graphene sheet and Ge(110) surface atoms was obtained in these calculations. The discussed experimental facts (possibility to measure LEED of the underlying reconstructed Ge(110) surface; measured height profile agrees with the theoretical value; possibility to discriminate between graphene and Ge(110) in STM experiments depending on the tunneling bias voltage) confirm our conclusion about the monolayer-thick graphene patches on Ge(110) in our samples.

Our atomically resolved STM images demonstrate clear signatures of quasiparticle scattering in the graphene layer due to imperfections in graphene as well as due to the presence of the scattering centres at the interface (segregated dopants, see discussion below). The interference of the scattering waves of the carriers in graphene leads to the formation of the corresponding $(\sqrt{3} \times \sqrt{3})R30^{\circ}$ structure with respect to the graphene atomic-related structure in the 2D Fast-Fourier-Transformation (FFT) map. The spots of these structures are marked in the upper inset of Fig. 1(e) by white rectangle and circle, respectively. This $(\sqrt{3} \times \sqrt{3})R30^{\circ}$ structure in the FFT map is assigned to the so-called intervalley scattering between adjacent cones at the *K* and *K′* points of the graphene-derived Brillouin zone.

The Raman spectrum of one of the gr/Ge(110) samples with an estimated graphene coverage of ≈50 – 60% is presented in Fig. 1(i). All graphene-related spectral features ("2D", "G", "D") are clearly resolved (the peak at 2329 cm^{-1} and the weak shoulder at 1556 cm^{-1} are due to atmospheric oxygen and nitrogen [23]). The 2D peak can be fitted with the single Lorentzian function: peak position 2725 cm^{-1} and FWHM = 65 cm^{-1}. The relatively low 2D/G intensity ratio indicates the formation of graphene patches on the Ge(110) surface. The observed high intensity of the D peak also hints towards the patch-like structure of our graphene sample on Ge(110) with a large contribution of the flake edges in the resulting Raman signal.

The formation of the uniform graphene sp^2 structure is also confirmed by XPS data (Fig. 2). High-temperature deposition of graphene on Ge(110) only leads to a damping of the Ge 2*p* XPS signal [Fig. 2(a and b)] without any indication of the formation of Ge–C bonds as can be concluded from the analysis of the Ge-related XPS peaks. Our data reveal a single C 1*s* peak for gr/Ge(110) with a small shoulder at a low binding energies (due to the possible bonds between carbon atoms and dopant atoms segregated at the interface) that confirms the homogeneity of the prepared gr/Ge(110) system.

The electronic structure of the grown graphene layer on Ge(110) was investigated by NE PES for the occupied valence band states below E_F and by C *K*-edge ELNES for the unoccupied states above E_F and these results are presented in Fig. 3(a and b), respectively. From the comparison of the PES spectrum of gr/Ge(110) with the one of a

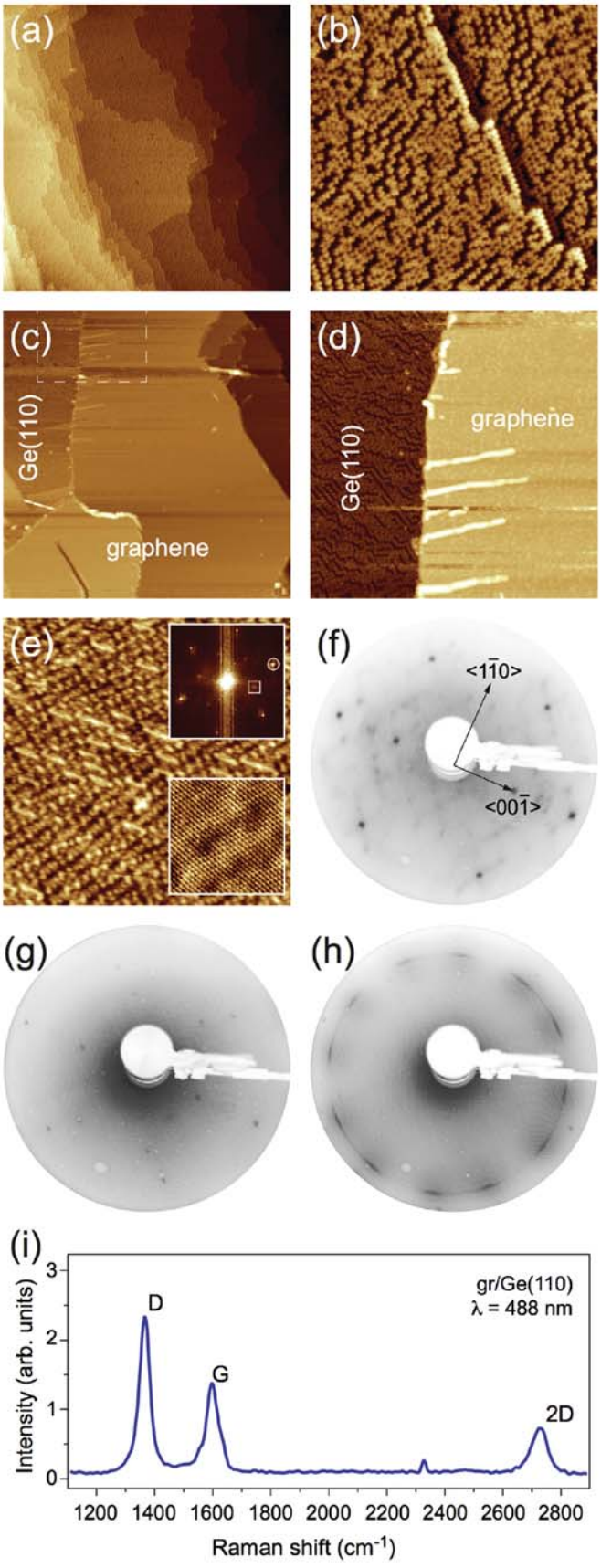

Fig. 1. STM and LEED characterization of Ge(110) (a,b,f) and gr/Ge(110) (c-e,g-h). The area marked by dashed rectangle in (c) is imaged with higher resolution in (d). The upper inset of (e) shows the corresponding FFT image of the STM data. White circle and rectangle mark the spots originating from graphene's atomic lattice and from the intervalley scattering in graphene, respectively. STM data were acquired at room temperature. Imaging parameters: (a) 500×500 nm^2, $U_T = +2.5$ V, $I_T = 1$ nA, (b) 80×80 nm^2, $U_T = +2.5$ V, $I_T = 0.3$ nA, (c) 400×400 nm^2, $U_T = +0.5$ V, $I_T = 5$ nA, (d) 150×150 nm^2, $U_T = +0.5$ V, $I_T = 6$ nA, (e) 30×30 nm^2, $U_T = +1.5$ V, $I_T = 0.8$ nA (inset: 7×7 nm^2, $U_T = +0.02$ V, $I_T = 8$ nA). Electron beam energy is 38 eV for (f,g) and 73 eV for (h), respectively. (i) Raman spectrum of gr/Ge(110). (A colour version of this figure can be viewed online.)

graphite single crystal, we can conclude that, in the former case the graphene-derived π and σ states are shifted towards higher binding energies by ≈ 1 eV and ≈ 0.5 eV, respectively. This shift indicates that in the present study the graphene layer is *n*-doped, which is opposite to the result presented in Ref. [29], where a small *p*-doping of graphene was observed with the position of the Dirac point of $E_D = 0.185$ eV above E_F. This difference can be attributed to the different types of substrates used in the experiments: *n*-doped (Sb) Ge(110) in the present study and an undoped Ge-epilayer on Si(001) in Ref. [29]. The cleaning procedure of Ge(110) (cycles of the Ar^+-sputtering and annealing) as well as the high temperature used during graphene growth can lead to the segregation of Sb atoms at the Ge(110) surface or/and their inclusion as dopants in the graphene layer, thus influencing the doping of the formed graphene layer. This is confirmed by our LT STM ($T = 24$ K) data of gr/Ge(110) which are presented as upper insets of Fig. 3(a), where one can clearly see the STM-signatures of the influence of dopant atoms on the scattering picture in the graphene layer (one of them is circled) [34–36]. Although the first ARPES data on Sb-atom adsorption on graphene/SiC pointed towards the possible *p*-doping of graphene [37], the recent theoretical works on Sb intercalation in gr/SiC reveal an *n*-doping of graphene [38]. A similar effect of *n*-doping of free-standing graphene upon Sb adsorption was also observed in experiment [39].

The unoccupied electronic states of graphene on Ge(110) were probed by the C *K*-edge ELNES spectroscopy, which can be considered as a simplified version of the near-edge x-ray absorption spectroscopy (NEXAFS). Here we used an electron beam of energy $E_p = 700$ eV and detected the signal originating from the energy losses due to the excitation of electrons from the C 1*s* core level of the carbon atoms in graphene onto the unoccupied states above E_F. Similar to NEXAFS this method is element-specific, i. e. the intensity of the loss-signal is proportional to the atom-projected partial density of unoccupied states of the elements in the system, the core-level of which is involved in the process. In our case we will observe two structures, which can be assigned to the $1s \rightarrow \pi^*$ and $1s \rightarrow \sigma^*$ transitions and the respective density of states above E_F [40–43].

The C *K*-edge ELNES spectrum of gr/Ge(110), collected in the specular-reflected electron-beam geometry, is shown in the lower part of [Fig. 3(b)] and compared with the theoretical ELNES (middle part) [44] and NEXAFS (upper part) [45] spectra of graphene and the gr/Ni(111) system. [All theoretical spectra were shifted by the same energy value in order to have the first peak, corresponding to the $1s \rightarrow \pi^*$ transition in the theoretical ELNES spectra, energetically coincide with the same peak in the experimental spectrum. The double-peak structure of the $1s \rightarrow \sigma^*$ transition in the NEXAFS spectrum is assigned to (i) an excitonic state close to the absorption threshold and described in the framework of the Mahan-Noziéres-De Dominicis (MND) theory and (ii) the nonexcitonic delocalized state, shifted by ≈ 1.4 eV with respect to the first line, the description of which is beyond the MND theory [46,47].] One can see that there is a very good agreement between the experimental ELNES spectrum of gr/Ge(110) and the theoretical ELNES spectrum for free-standing graphene (lower and middle parts): (i) both $1s \rightarrow \pi^*$ and $1s \rightarrow \sigma^*$ transitions exhibit a single peak at the respective threshold,

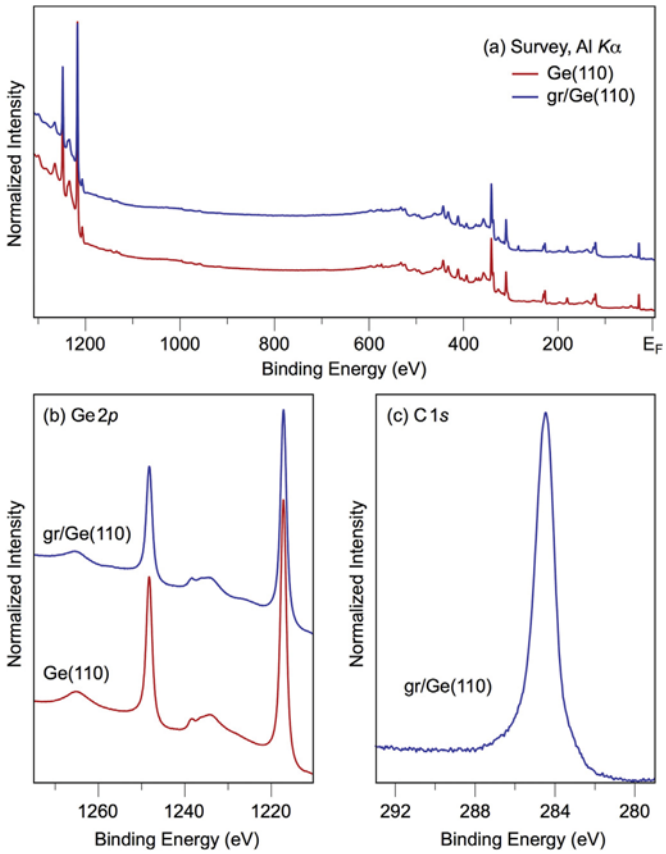

Fig. 2. XPS spectra of Ge(110) and gr/Ge(110): (a) surveys, (b) Ge 2*p*, and (c) C 1*s*. (A colour version of this figure can be viewed online.)

that can be interpreted as a signature of the weak interaction between graphene and the Ge(110) surface, (ii) the energy splitting between two transitions in the experimental spectrum is almost

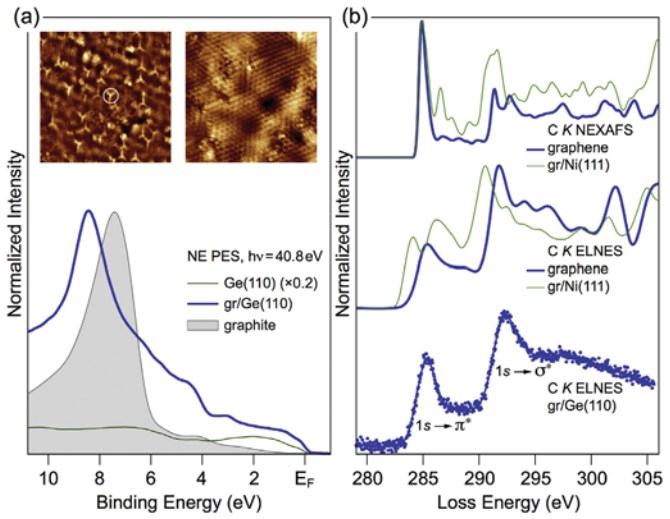

Fig. 3. (a) NE PES spectra of Ge(110) (intensity is scaled down by factor 5) and gr/Ge(110). The spectrum of the crystal is shown as a shaded area for comparison. The inset shows LT STM images of gr/Ge(110), where scattering features due to dopant atoms are clearly resolved. Imaging parameters: (left) 20×20 nm^2, $U_T = +1.0$ V, $I_T = 0.2$ nA, (right) 10×10 nm^2, $U_T = +0.5$ V, $I_T = 0.9$ nA. (b) Experimental and theoretical C *K*-edge ELNES and NEXAFS spectra of gr/Ge(110), graphene, and gr/Ni(111). (A colour version of this figure can be viewed online.)

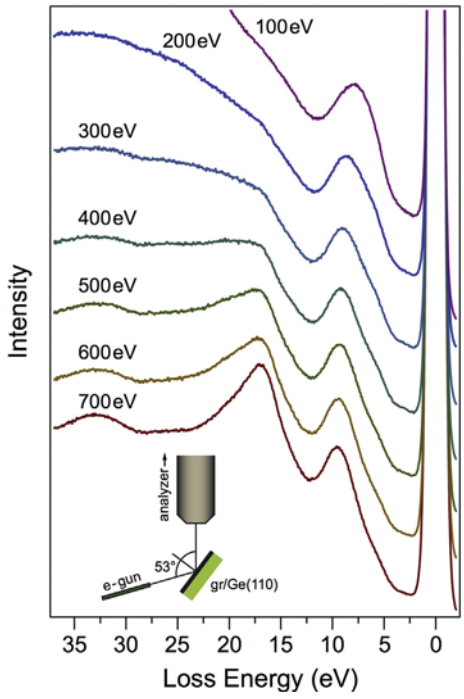

Fig. 4. EELS spectra of gr/Ge(110) obtained with different primary beam energies. The energy of the electron beam is marked for every spectrum. Lower inset presents the geometry used in the EELS/ELNES experiments. (A colour version of this figure can be viewed online.)

identical to the one deduced from the theoretically calculated ELNES spectrum. As was shown in Refs. [44,45,48,49], the value of this splitting as well as the modification of the shape of the $1s \rightarrow \pi^*$ transition can be taken as an indication for the $sp^2 - sp^3$ rehybridization of carbon atoms, which can appear due to the contact of graphene with the substrate or due to the adsorption of different species on top of graphene [7]. Such an example of the spectral shape modifications of the ELNES and NEXAFS spectra for the *strongly* interacting gr/Ni(111) interface is shown in Fig. 3(b). As was presented, besides the strong *n*-doping of graphene on Ni, there is also a substantial intermixing of the valence band states of graphene and Ni, leading to a strong modification of the energy distribution of the partial density of states of both elements. All discussed effects are clearly visible in ELNES as well as in the NEXAFS spectra, due to the similarity of the electron excitation processes.

In our EELS experiments on gr/Ge(110), we also address the plasmon excitations in the system. Fig. 4 shows the energy-loss spectra for this system measured as a function of the primary electron beam energy (marked for every spectrum) and presented in the energy range around the elastic peak (zero energy-loss energy). These spectra reveal a series of peaks ($\approx$17 eV, $\approx$33 eV), which can be clearly assigned to bulk Ge plasmons, whereas the peak at $\approx$9.5 eV and the low energy shoulders can be assigned to surface-related transitions of Ge(110) [50–53].

A variation of the primary beam energy allows to change the surface sensitivity of EELS as can be seen from Fig. 4. This leads to an increase of the graphene-related signal in the EELS spectra as the energy of the electron beam decreases, which manifests itself as an increase in intensity within the energy range of 3.5 – 6.5 eV as well as an increase of the overall background for the energies above 15 eV. The first feature is assigned to the so-called π plasmon [54–56], the energy of which is determined as 6.33±0.25 eV by a curve fitting procedure. The second feature is connected to an increase of the intensity of the $\pi + \sigma$ plasmon as well as the increase

of the background of the low energy inelastically scattered electrons. The exact position of the $\pi + \sigma$ plasmon cannot be extracted from these data.

4. Conclusions

In conclusion, we demonstrate the growth of a high-quality graphene layer on Ge(110) by evaporation of atomic carbon on a hot Ge surface. Our STM and LEED data confirm the honeycomb sp^2 structure of the graphene layer. From the analysis of the electronic structure of the graphene layer by means of PES and ELNES we conclude the nearly free-standing character of graphene which was found to be *n*-doped due to the segregation of Sb dopant atoms at the gr/Ge interface during sample preparation routines. Such an effect of the substrate-dopant segregation at the graphene-semiconductor interface can be used for a controllable doping of graphene that might influence its electron- and spin-transport properties. Our and earlier results demonstrate the perspective of the use of Ge(110) [or presently available epi-Ge(110)/Si(110) substrates] for the synthesis of high-quality weakly-bonded to substrate graphene from an atomic carbon source. The standard preparation routine used for Si or Ge substrates might be easily adapted here. Such graphene growth does not cause the strong restructuring or faceting of the underlying Ge surface, as it is found for the case of Ge(001). However, the fabrication of Ge(110)/Si(110) with the quality comparable to the one for (001)-oriented wafers might limit the adaptation of this method in semiconducting technology.

Acknowledgement

We thank the German Research Foundation (DFG) for financial support within the Priority Programme 1459 “Graphene” We further gratefully acknowledge the assistance of Axel Herguth (AG Photovoltaik, Universität Konstanz) with the Raman spectra measurements.

References

[1] C. Virojanadara, M. Syvaejarvi, R. Yakimova, L.I. Johansson, A.A. Zakharov, T. Balasubramanian, Homogeneous large-area graphene layer growth on 6H-SiC(0001), Phys. Rev. B 78 (2008) 245403.
[2] K.V. Emtsev, A. Bostwick, K. Horn, J. Jobst, G.L. Kellogg, L. Ley, J.L. McChesney, T. Ohta, S.A. Reshanov, J. Roehrl, E. Rotenberg, A.K. Schmid, D. Waldmann, H.B. Weber, T. Seyller, Towards wafer-size graphene layers by atmospheric pressure graphitization of silicon carbide, Nat. Mater. 8 (2009) 203–207.
[3] M. Sprinkle, M. Ruan, Y. Hu, J. Hankinson, M. Rubio-Roy, B. Zhang, X. Wu, C. Berger, W.A. De Heer, Scalable templated growth of graphene nanoribbons on SiC, Nat. Nanotechnol. 5 (2010) 727–731.
[4] X. Li, W. Cai, J. An, S. Kim, J. Nah, D. Yang, R. Piner, A. Velamakanni, I. Jung, E. Tutuc, S.K. Banerjee, L. Colombo, R.S. Ruoff, Large-area synthesis of high-quality and uniform graphene films on copper foils, Science 324 (2009) 1312–1314.
[5] S. Bae, H. Kim, Y. Lee, X. Xu, J.-S. Park, Y. Zheng, J. Balakrishnan, T. Lei, H.R. Kim, Y.I. Song, Y.-J. Kim, K.S. Kim, B. Ozyilmaz, J.-H. Ahn, B.H. Hong, S. Iijima, Roll-to-roll production of 30-inch graphene films for transparent electrodes, Nat. Nanotechnol. 5 (2010) 574–578.
[6] L. Tao, J. Lee, M. Holt, H. Chou, S.J. McDonnell, D.A. Ferrer, M.G. Babenco, R.M. Wallace, S.K. Banerjee, R.S. Ruoff, Uniform wafer-scale chemical vapor deposition of graphene on evaporated Cu (111) film with quality comparable to exfoliated monolayer, J. Phys. Chem. C 116 (2012) 24068–24074.
[7] Y. Dedkov, E. Voloshina, Graphene growth and properties on metal substrates, J. Phys.: Condens. Matter 27 (2015) 303002.
[8] M. Kruskopf, D.M. Pakdehi, K. Pierz, S. Wundrack, R. Stosch, Th. Dziomba, M. Götz, J. Baringhaus, J. Aprojanz, C. Tegenkamp, J. Lidzba, Th. Seyller, F. Hohls, F.J. Ahlers, H.W. Schumacher, Comeback of epitaxial graphene for electronics: large-area growth of bilayer-free graphene on SiC, 2D Mater. 3 (2016) 041002.
[9] A. Ambrosi, M. Pumera, The CVD graphene transfer procedure introduces metallic impurities which alter the graphene electrochemical properties, Nanoscale 6 (2014) 472–476.
[10] G. Lupina, J. Kitzmann, I. Costina, M. Lukosius, C. Wenger, A. Wolff, S. Vaziri, M. Östling, I. Pasternak, A. Krajewska, W. Strupinski, S. Kataria, A. Gahoi, M.C. Lemme, G. Ruhl, G. Zoth, O. Luxenhofer, W. Mehr, Residual metallic contamination of transferred chemical vapor deposited graphene, ACS Nano 9 (5) (2015) 4776–4785.
[11] M. Peplow, Graphene booms in factories but lacks a killer app, Nature 522 (2015) 268–269.
[12] S. Park, The puzzle of graphene commercialization, Nat. Rev. Mater. 1 (2016) 16085.
[13] J.H. Meng, X.W. Zhang, H.L. Wang, X.B. Ren, C.H. Jin, Z.G. Yin, X. Liu, H. Liu, Synthesis of in-plane and stacked graphene/hexagonal boron nitride heterostructures by combining with ion beam sputtering deposition and chemical vapor deposition, Nanoscale 7 (2015) 16046–16053.
[14] S.M. Kim, A. Hsu, M.-H. Park, S.H. Chae, S.J. Yun, J.S. Lee, D.-H. Cho, W. Fang, C. Lee, T. Palacios, M. Dresselhaus, K.K. Kim, Y.H. Lee, J. Kong, Synthesis of large-area multilayer hexagonal boron nitride for high material performance, Nat. Commun. 6 (2015) 8662.
[15] J. Yin, X. Liu, W. Lu, J. Li, Y. Cao, Y. Li, Y. Xu, X. Li, J. Zhou, C. Jin, W. Guo, Aligned growth of hexagonal boron nitride monolayer on germanium, Small 11 (2015) 5375–5380.
[16] Q. Liu, Y. Gong, T. Wang, W.-L. Chan, J. Wu, Metal-catalyst-free and controllable growth of high-quality monolayer and AB-stacked bilayer graphene on silicon dioxide, Carbon 96 (2016) 203–211.
[17] J. Hackley, D. Ali, J. DiPasquale, J.D. Demaree, C.J.K. Richardson, Graphitic carbon growth on Si(111) using solid source molecular beam epitaxy, Appl. Phys. Lett. 95 (2009) 133114.
[18] M. Suemitsu, H. Fukidome, Epitaxial graphene on silicon substrates, J. Phys. D 43 (2010) 374012.
[19] F. Maeda, H. Hibino, Study of graphene growth by gas-source molecular beam epitaxy using cracked ethanol: influence of gas flow rate on graphitic material deposition, Jpn. J. Appl. Phys. 50 (2011), 06GE12.
[20] G. Hong, Q.-H. Wu, J. Ren, S.-T. Lee, Mechanism of non-metal catalytic growth of graphene on silicon, Appl. Phys. Lett. 100 (2012) 231604.
[21] P. Thanh Trung, J. Campos-Delgado, F. Joucken, J.-F. Colomer, B. Hackens, J.-P. Raskin, C.N. Santos, S. Robert, Direct growth of graphene on Si(111), J. Appl. Phys. 115 (2014) 223704.
[22] J.-H. Lee, E.K. Lee, W.-J. Joo, Y. Jang, B.-S. Kim, J.Y. Lim, S.-H. Choi, S.J. Ahn, J.R. Ahn, M.-H. Park, C.-W. Yang, B.L. Choi, S.W. Hwang, D. Whang, Wafer-scale growth of single-crystal monolayer graphene on reusable hydrogen-terminated germanium, Science 344 (2014) 286–289.
[23] G. Lippert, J. Dabrowski, T. Schroeder, M.A. Schubert, Y. Yamamoto, F. Herziger, J. Maultzsch, J. Baringhaus, C. Tegenkamp, M.C. Asensio, J. Avila, G. Lupina, Graphene grown on Ge(001) from atomic source, Carbon 75 (2014) 104–112.
[24] P.C. Rogge, M.E. Foster, J.M. Wofford, K.F. McCarty, N.C. Bartelt, O.D. Dubon, On the rotational alignment of graphene domains grown on Ge(110) and Ge(111), MRS Commun. 5 (2015) 539–546.
[25] B. Kiraly, R.M. Jacobberger, A.J. Mannix, G.P. Campbell, M.J. Bedzyk, M.S. Arnold, M.C. Hersam, N.P. Guisinger, Electronic and mechanical properties of graphene–germanium interfaces grown by chemical vapor deposition, Nano Lett. 15 (2015) 7414–7420.
[26] A.M. Scaparro, V. Miseikis, C. Coletti, A. Notargiacomo, M. Pea, M. De Seta, L. Di Gaspare, Investigating the CVD synthesis of graphene on Ge(100): toward layer-by-layer growth, ACS Appl. Mater. Interfaces 8 (2016) 33083–33090.
[27] R.M. Jacobberger, B. Kiraly, M. Fortin-Deschenes, P.L. Lévesque, K.M. McElhinny, G.J. Brady, R.R. Delgado, S.S. Roy, A. Mannix, M.G. Lagally, P.G. Evans, P. Desjardins, R. Martel, M.C. Hersam, N.P. Guisinger, M.S. Arnold, Direct oriented growth of armchair graphene nanoribbons on germanium, Nat. Commun. 6 (2015) 8006.
[28] M. Lukosius, J. Dabrowski, J. Kitzmann, O. Fursenko, F. Akhtar, M. Lisker, G. Lippert, S. Schulze, Y. Yamamoto, M.A. Schubert, H.M. Krause, A. Wolff, A. Mai, T. Schroeder, G. Lupina, Metal-free CVD graphene synthesis on 200 mm Ge/Si(001) substrates, ACS Appl. Mater. Interfaces 8 (2016) 33786–33793.
[29] J. Dabrowski, G. Lippert, J. Avila, J. Baringhaus, I. Colambo, Y.S. Dedkov, F. Herziger, G. Lupina, J. Maultzsch, T. Schaffus, T. Schroeder, M. Kot, C. Tegenkamp, D. Vignaud, M.C. Asensio, Understanding the growth mechanism of graphene on Ge/Si(001) surfaces, Sci. Rep. 6 (2016) 31639.
[30] B.Z. Olshanetsky, S.M. Repinsky, A.A. Shklyaev, LEED investigation of germanium surfaces cleaned by sublimation of sulphide films; structural transitions on clean Ge(110) surface, Surf. Sci. 64 (1977) 224–236.
[31] T. Ichikawa, In situ STM observations of ordering behaviors on Ge(110) surfaces and atomic geometry of the Ge{17 15 1} facet, Surf. Sci. 560 (2004) 213–225.
[32] T. Ichikawa, Atomic geometry of the Ge(110)$c(8 \times 10)$ structure, Surf. Sci. 560 (2004) 205–212.
[33] C.H. Mullet, S. Chiang, Reconstructions and phase transition of clean Ge(110), Surf. Sci. 621 (2014) 184–190.
[34] L. Zhao, R. He, K.T. Rim, T. Schiros, K.S. Kim, H. Zhou, Ch. Gutiérrez, S.P. Chockalingam, C.J. Arguello, L. Pálová, D. Nordlund, M.S. Hybertsen, D.R. Reichman, T.F. Heinz, P. Kim, A. Pinczuk, G.W. Flynn, A.N. Pasupathy, Visualizing individual nitrogen dopants in monolayer graphene, Science 333 (2011) 999–1003.
[35] Y. Tison, J. Lagoute, V. Repain, C. Chacon, Y. Girard, S. Rousset, F. Joucken, D. Sharma, L. Henrard, H. Amara, A. Ghedjatti, F. Ducastelle, Electronic interaction between nitrogen atoms in doped graphene, ACS Nano 9 (2015) 670–678.

[36] F. Joucken, Y. Tison, P. Le Févre, A. Tejeda, A. Taleb-Ibrahimi, E. Conrad, V. Repain, C. Chacon, A. Bellec, Y. Girard, S. Rousset, J. Ghijsen, R. Sporken, H. Amara, F. Ducastelle, J. Lagoute, Charge transfer and electronic doping in nitrogen-doped graphene, Sci. Rep. 5 (2015) 14564.
[37] I. Gierz, C. Riedl, U. Starke, C. Ast, K. Kern, Atomic hole doping of graphene, Nano Lett. 8 (2008) 4603–4607.
[38] C.-H. Hsu, V. Ozolins, F.-C. Chuang, First-principles study of Bi and Sb intercalated graphene on SiC(0001) substrate, Surf. Sci. 616 (2013) 149–154.
[39] H.M.W. Khalil, J.T. Nam, K.S. Kim, H. Noh, Controlled n-doping in chemical vapour deposition grown graphene by antimony, J. Phys. D 48 (2015) 015307.
[40] K. Suenaga, E. Sandré, C. Colliex, C.J. Pickard, H. Kataura, S. Iijima, Electron energy-loss spectroscopy of electron states in isolated carbon nanostructures, Phys. Rev. B 63 (2001), 165408–4.
[41] J.T. Titantah, D. Lamoen, Energy-loss near-edge structure changes with bond length in carbon systems, Phys. Rev. B 72 (2005), 193104–4.
[42] K.A. Mkhoyan, A.W. Contryman, J. Silcox, D.A. Stewart, G. Eda, C. Mattevi, S. Miller, M. Chhowalla, Atomic and electronic structure of graphene-oxide, Nano Lett. 9 (2009) 1058–1063.
[43] A. Cupolillo, N. Ligato, S.M. Osman, L.S. Caputi, Carbon *K*-edge electron-energy-loss near-edge structure in the reflection mode on graphene/Ni(111), Appl. Phys. Lett. 109 (2016) 161603–161606.
[44] G. Bertoni, L. Calmels, A. Altibelli, V. Serin, First-principles calculation of the electronic structure and EELS spectra at the graphene/Ni(111) interface, Phys. Rev. B 71 (2004) 075402.
[45] E. Voloshina, R. Ovcharenko, A. Shulakov, Y. Dedkov, Theoretical description of X-ray absorption spectroscopy of the graphene-metal interfaces, J. Chem. Phys. 138 (2013) 154706.
[46] O. Wessely, M.I. Katsnelson, O. Eriksson, *Ab initio* theory of dynamical core-hole screening in graphite from x-ray absorption spectra, Phys. Rev. Lett. 94 (2005) 167401.
[47] O. Wessely, O. Eriksson, M.I. Katsnelson, Dynamical core-hole screening in the x-ray absorption spectra of graphite, C_{60}, and carbon nanotubes: a first-principles electronic structure study, Phys. Rev. B 73 (2006) 075402.
[48] M. Weser, Y. Rehder, K. Horn, M. Sicot, M. Fonin, A.B. Preobrajenski, E.N. Voloshina, E. Goering, Y.S. Dedkov, Induced magnetism of carbon atoms at the graphene/Ni(111) interface, Appl. Phys. Lett. 96 (2010) 012504.
[49] J. Rusz, A.B. Preobrajenski, M.L. Ng, N.A. Vinogradov, N. Mårtensson, O. Wessely, B. Sanyal, O. Eriksson, Dynamical effects in x-ray absorption spectra of graphene and monolayered h-BN on Ni(111), Phys. Rev. B 81 (2010) 073402.
[50] R. Ludeke, L. Esaki, Electron energy-loss spectroscopy of GaAs and Ge surfaces, Phys. Rev. Lett. 33 (1974) 653–656.
[51] R. Ludeke, A. Koma, Low-energy-electron-loss spectroscopy of Ge surfaces, Phys. Rev. B 13 (1976) 739–749.
[52] X.J. Zhang, G. Xue, A. Agarwal, R. Tsu, M.A. Hasan, J.E. Greene, A. Rockett, Thermal desorption of ultraviolet–ozone oxidized Ge(001) for substrate cleaning, J. Vac. Sci. Technol. A 11 (1993) 2553–2561.
[53] L. Pasquali, S. D'Addato, L. Tagliavini, A.M. Prandini, S. Nannarone, Surface phase transitions of Ge(111)$c(2\times8)$ studied by electron energy loss spectroscopy, Surf. Sci. 377–379 (1997) 534–538.
[54] J. Lu, K. Loh, H. Huang, W. Chen, A. Wee, Plasmon dispersion on epitaxial graphene studied using high-resolution electron energy-loss spectroscopy, Phys. Rev. B 80 (2009) 113410.
[55] A. Politano, G. Chiarello, Plasmon modes in graphene: status and prospect, Nanoscale 6 (2014) 10927–10940.
[56] A. Politano, I. Radović, D. Borka, Z.L. Mišković, G. Chiarello, Interband plasmons in supported graphene on metal substrates: theory and experiments, Carbon 96 (2016) 91–97.